

Monitoring an oil-sands reservoir in northwest Alberta using time-lapse 3D seismic and 3D P-SV converted-wave data

TORU NAKAYAMA and AKIHISA TAKAHASHI, JAPEx, Tokyo, Japan

LEIGH SKINNER, JACOS, Calgary, Canada

AYATO KATO, University of Houston, USA

Time-lapse 3D seismic monitoring was conducted in the Japan Canada Oil Sands Limited (JACOS) Hangingstone steam-assisted-gravity-drainage (SAGD) operation area in Alberta, Canada, to delineate steam-affected areas. The time-lapse surveys, acquired in February 2002 and March 2006, show distinct response changes around the SAGD well pairs. In addition, 3D P-SV converted-wave processing and analysis were applied on the second 3D data set (recorded with three-component digital sensors) for a reservoir characterization study.

Background information on the Hangingstone SAGD operation is contained in the related article by Kato et al. in this *TLE* special section.

Time-lapse 3D seismic data.

Figure 1 shows a map of the two 3D seismic surveys and SAGD well locations in the field. Black solid lines represent SAGD well paths, and the red dotted line indicates a north-south line (referred as NS hereafter), which will be used

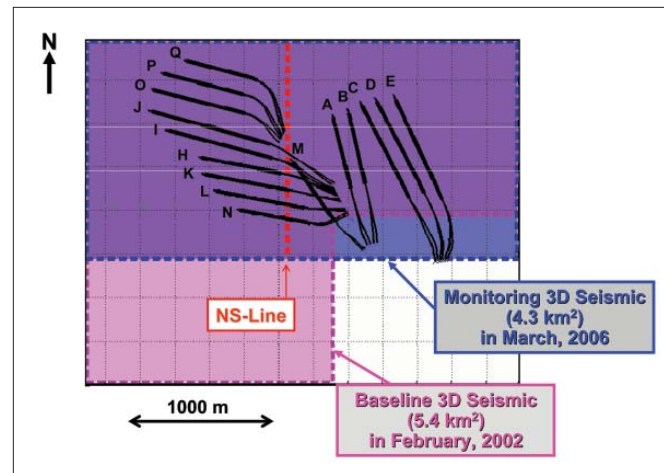
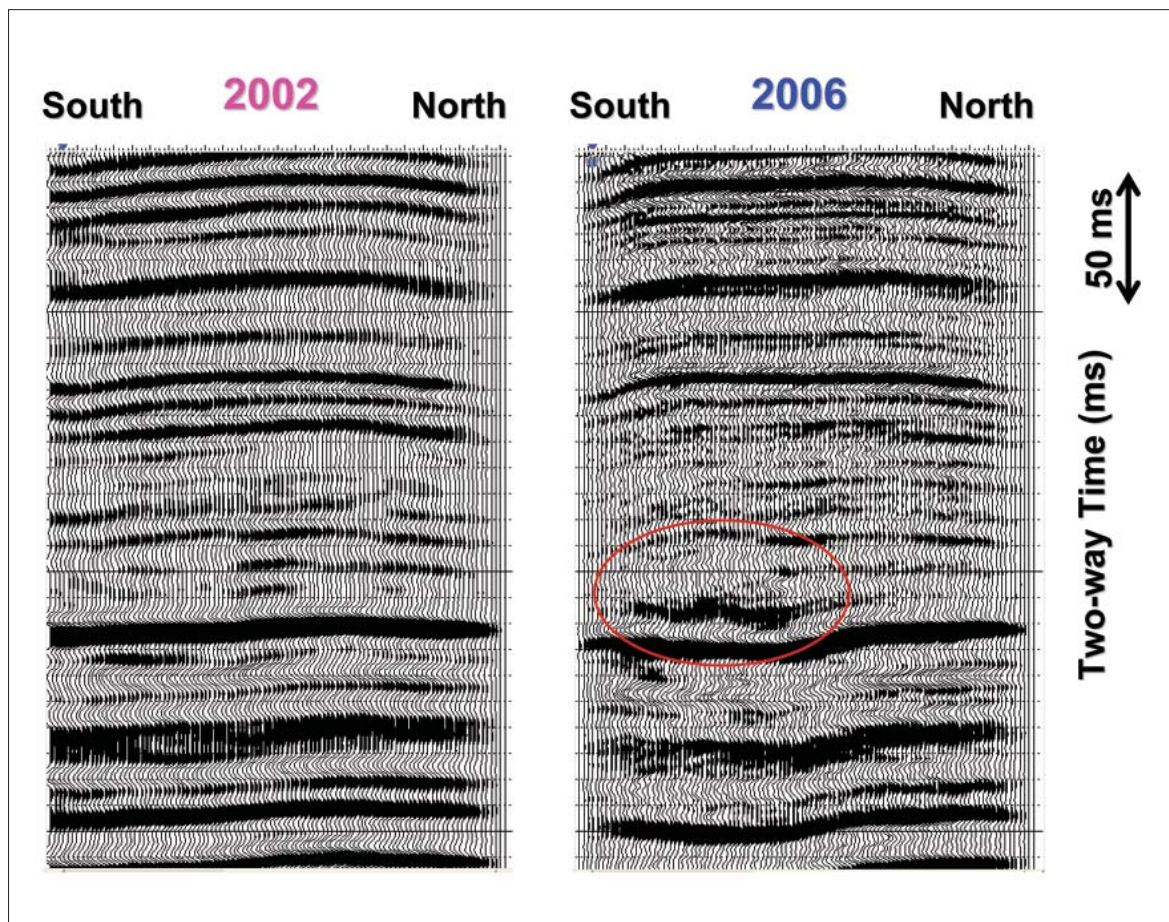


Figure 1. Map of the time-lapse 3D seismic survey and the SAGD well locations. Black solid lines represent SAGD well paths. The red dotted line shows the location of a representative north-south seismic section described in Figures 2, 3, 4, and 6.

Figure 2. Migrated sections (NS line) for the 2002 and 2006 surveys to which calibration has not been applied. The southern half of each section intersects with the SAGD well pairs H, I, K, L, M, and N. The northern part is away from the steam-injected areas.



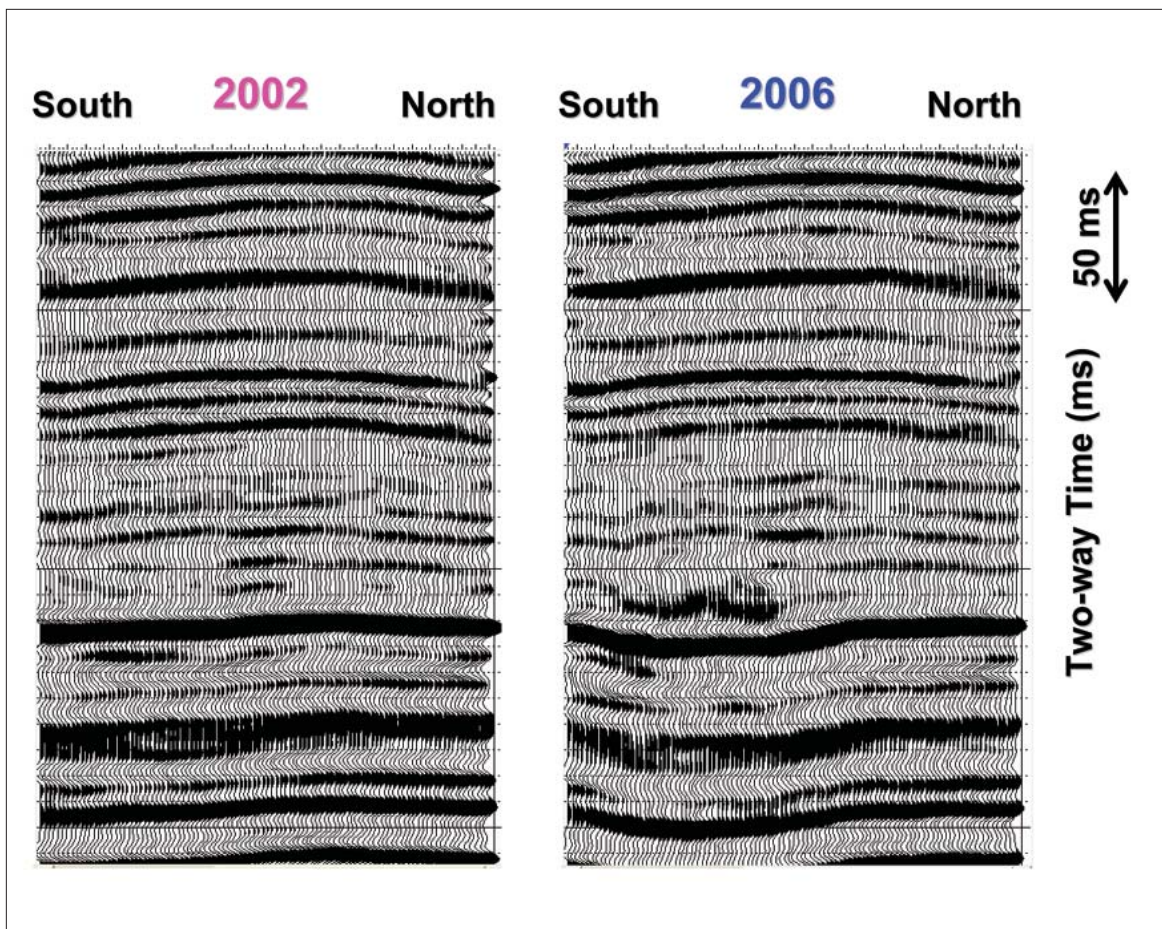


Figure 3. Sections from the calibrated 2006 data and the 2002 data.

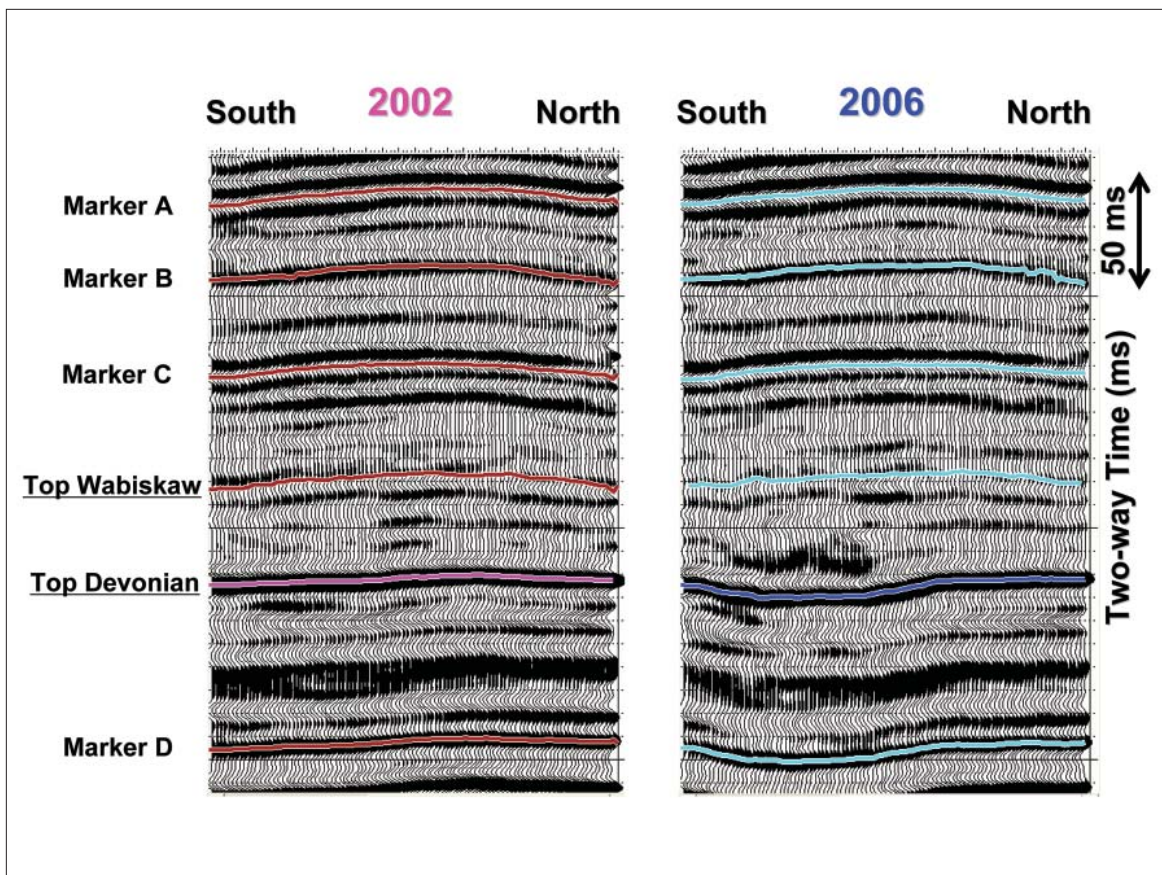
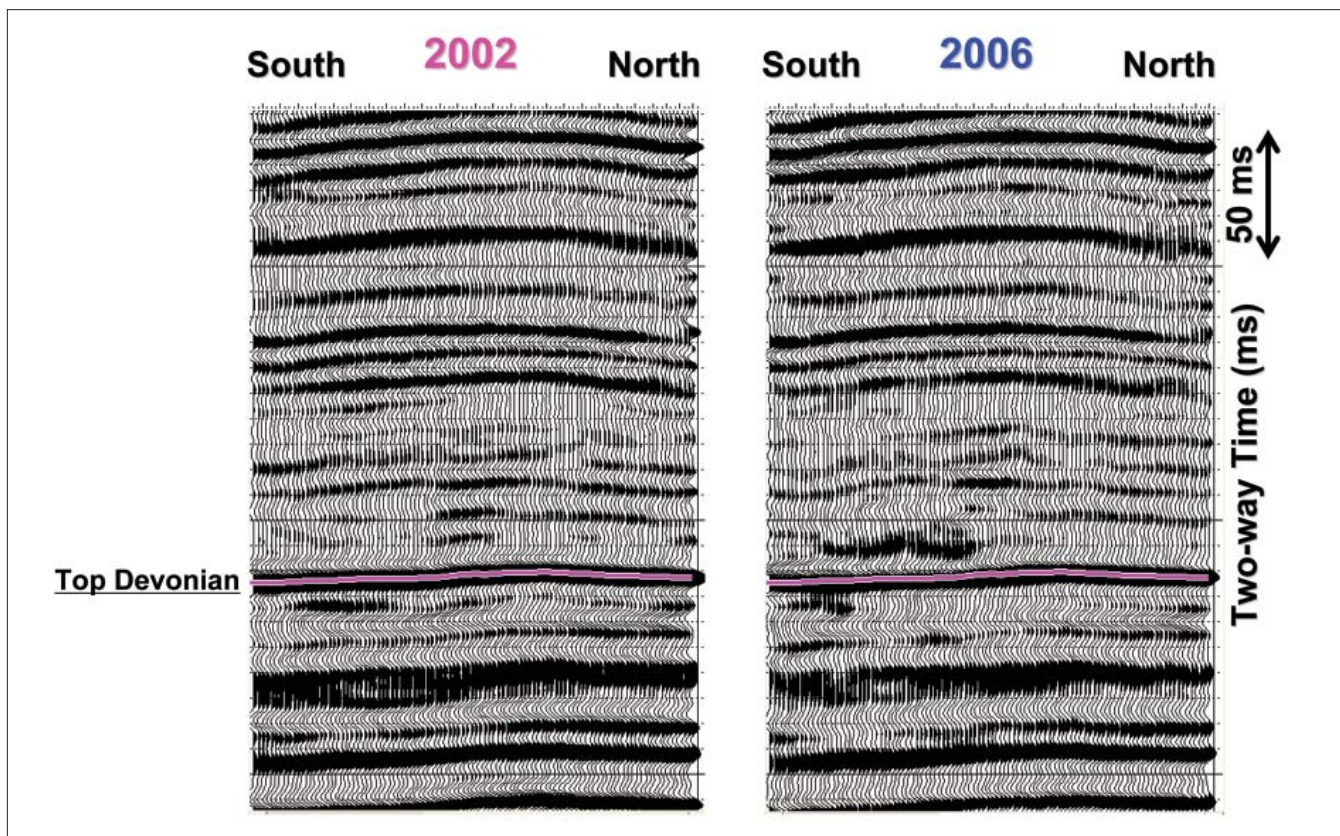
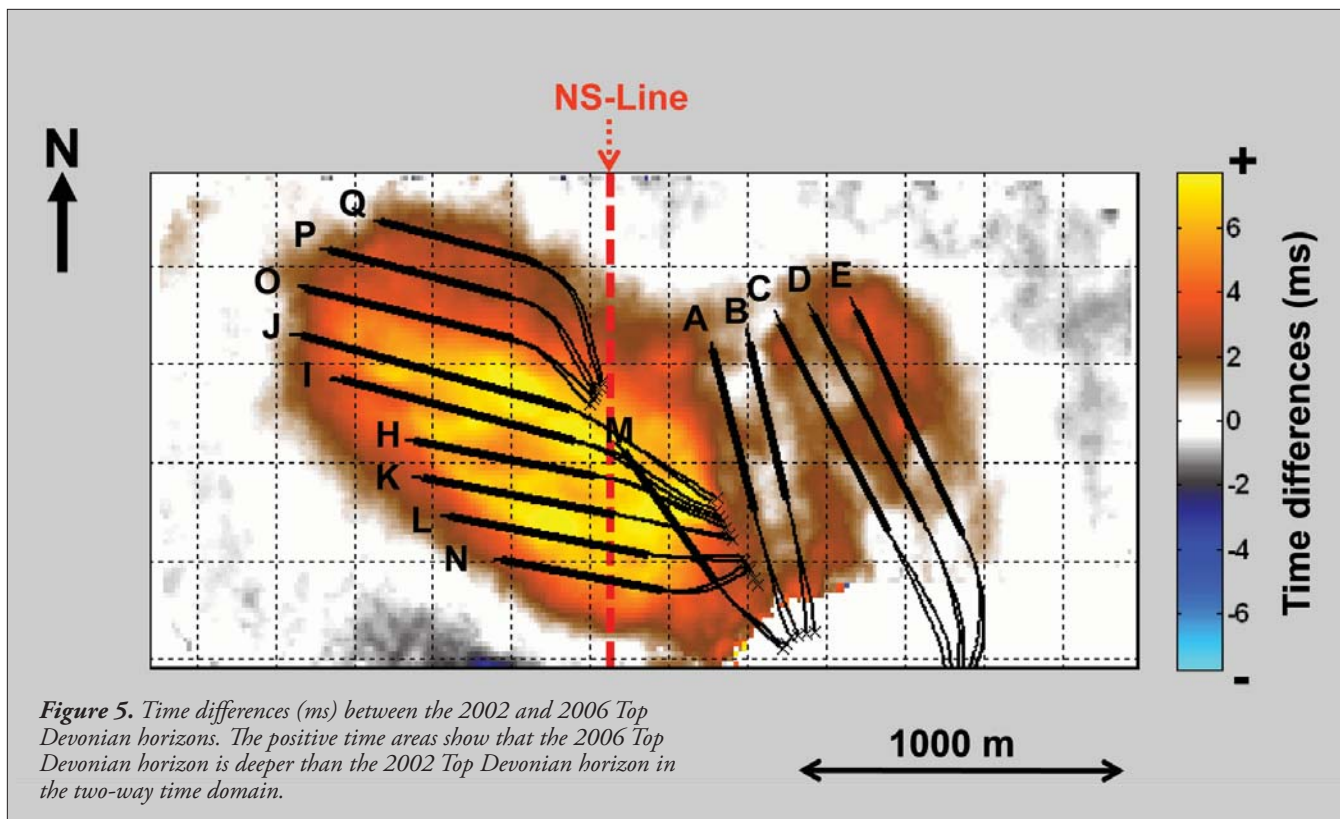
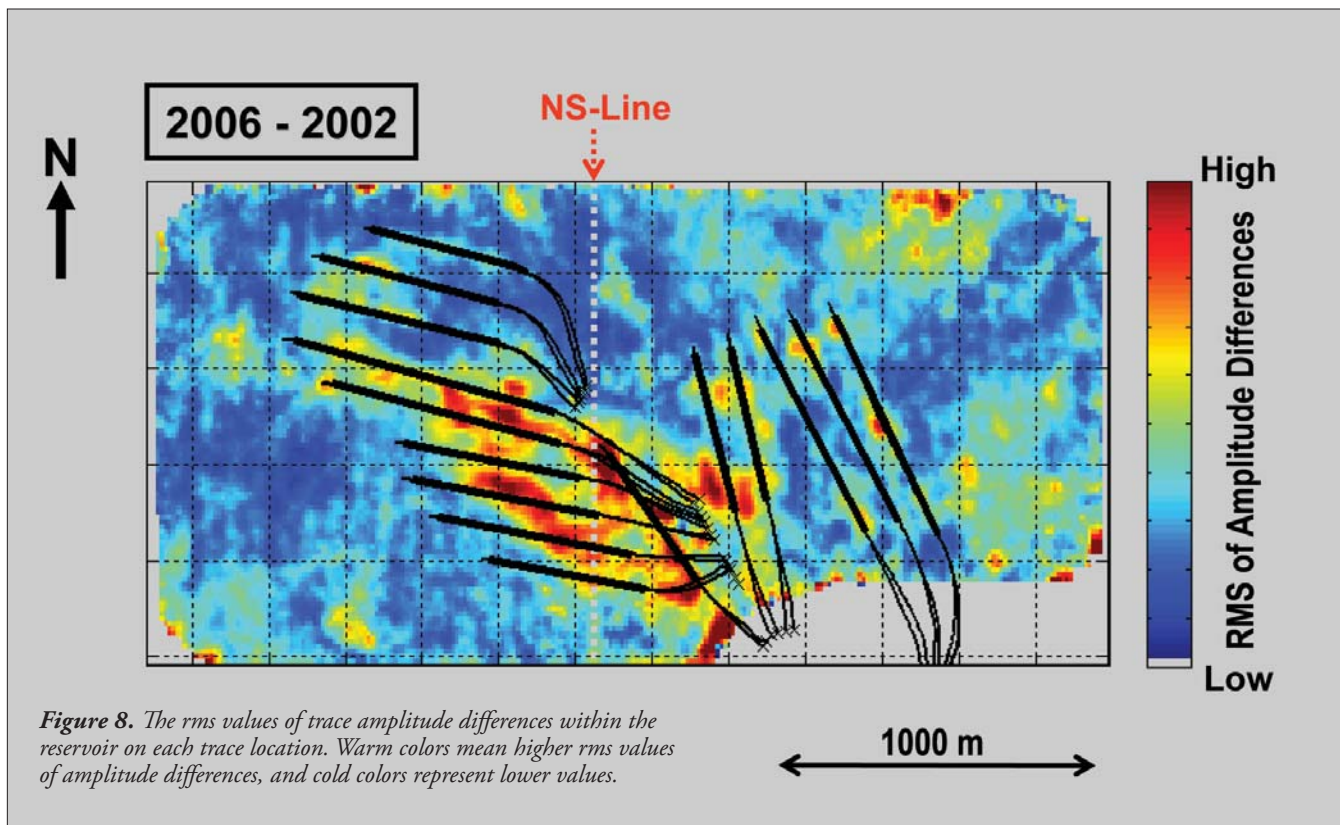
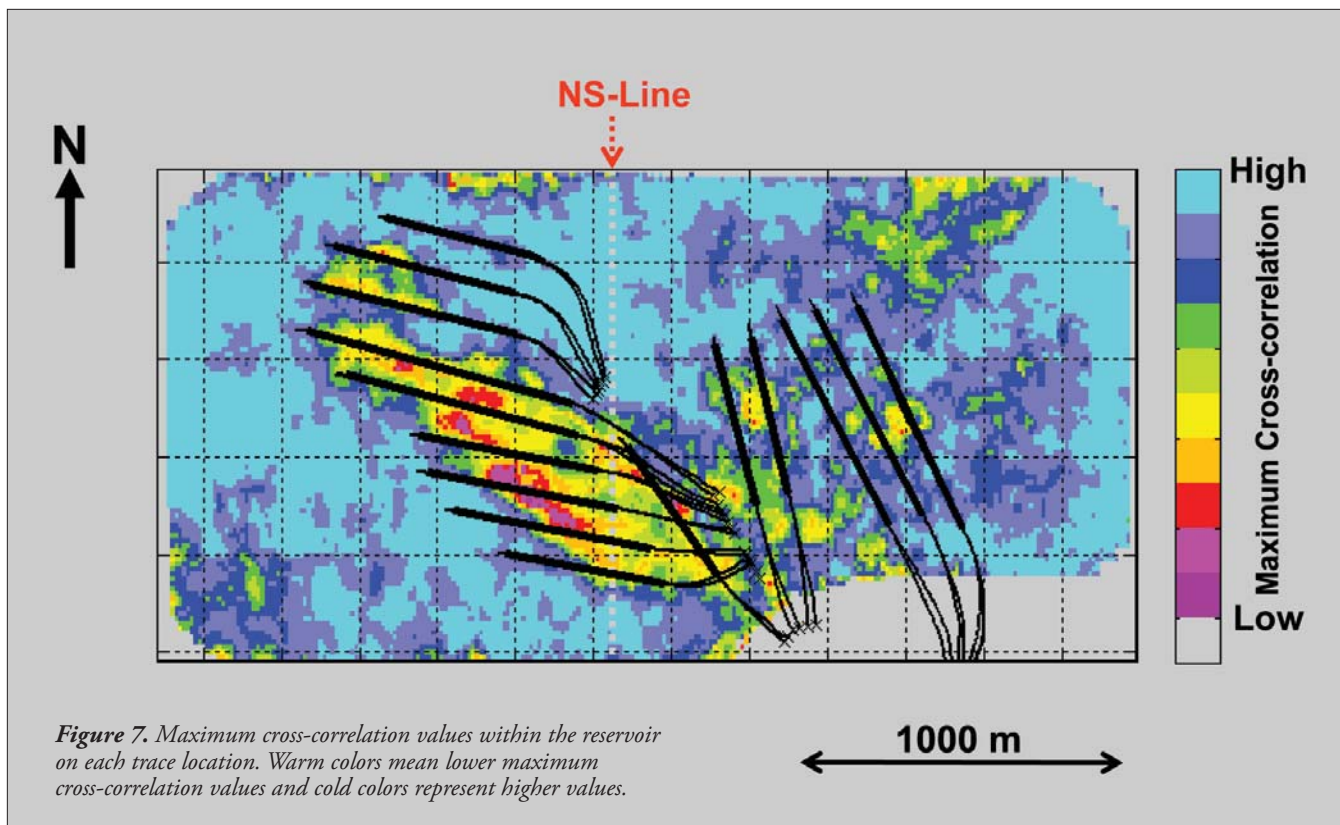


Figure 4. Interpreted NS line. Top Devonian is regarded as the reservoir bottom (Base McMurray) and Top Wabiskaw is about 5 m shallower than the reservoir top (Top McMurray).





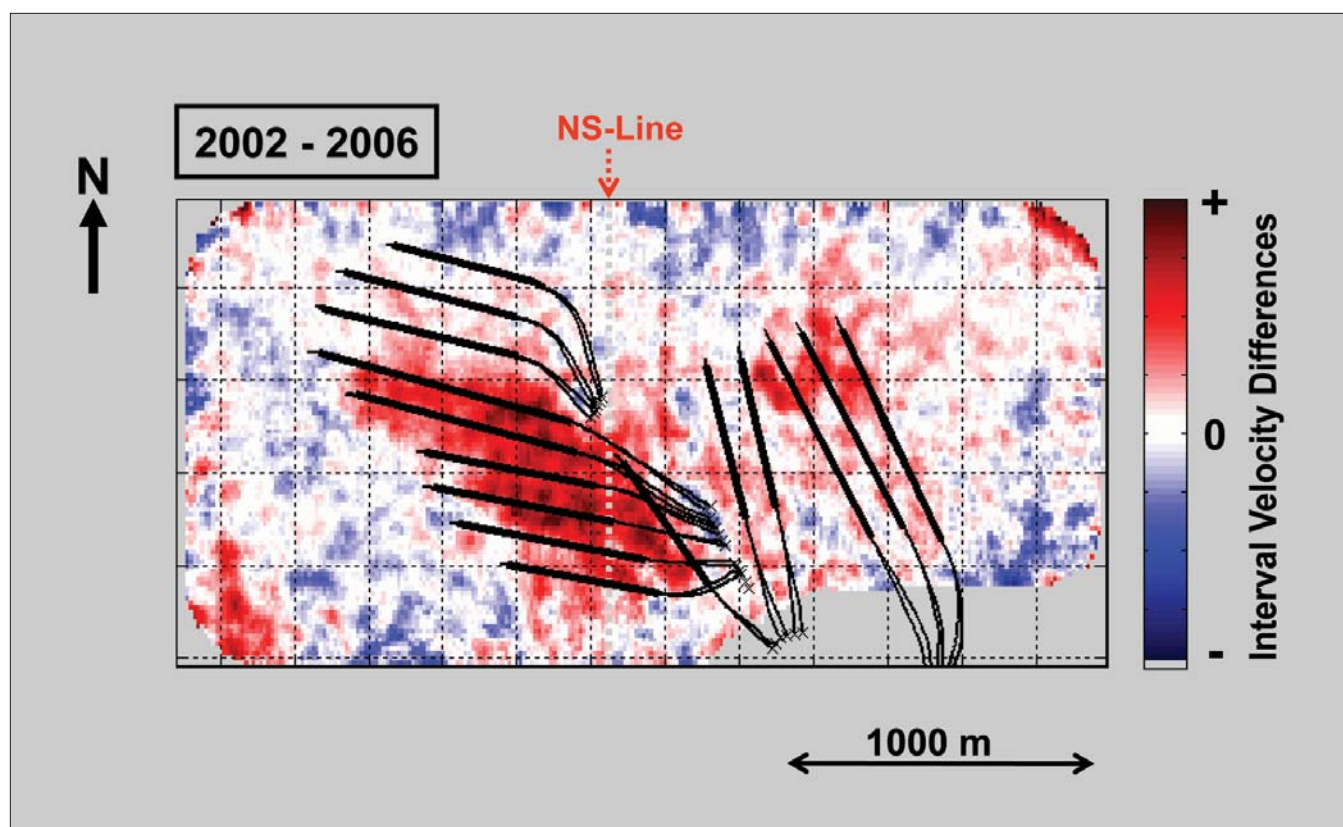


Figure 9. Interval velocity differences between time slices extracted from the smoothed 2002 and 2006 interval velocity cubes. The red areas (positive values) show that the interval velocities in 2006 are lower than those in 2002. This time slice intersects with the reservoir interval. The velocity data picked at every CMP location were smoothed to eliminate the erroneous values and then converted into the interval velocity cubes.

throughout this study. The first 3D seismic (baseline survey = 5.4 km²) was acquired in 2002 to construct detailed 3D geologic models for reservoir characterization. The production of the five eastern SAGD well pairs (A, B, C, D, and E in Figure 1) had already started when the survey was recorded. After the first 3D survey, steam injection was implemented in four stages at ten additional western SAGD well pairs prior to 2006. The second 3D survey was conducted in 2006 in the northern part (4.3 km²) of the 2002 baseline survey, where the active 15 SAGD wells exist.

The seismic data sets were recorded with nearly identical field acquisition parameters. One major difference between the surveys is the receiver type; analog geophone arrays were used in 2002 and three-component digital sensors were used in 2006.

Both data sets underwent an identical processing flow at the same time. In addition to the basic seismic data processing, spectral decomposition for the both surveys and P-SV data processing of the three-component monitoring survey were conducted.

Core velocity data and rock physics model

As described in the companion article by Kato et al., P- and S-wave velocities of oil sand core plugs from the field were measured under various pressure and temperature conditions in order to understand the relationship between elastic properties of the oil sands and changes in temperature and pore pressure.

As a result, a rock physics model was proposed to predict velocity changes of the oil sands caused by any variations of pore pressure, temperature, fluid saturation and fluid phase changes expected during SAGD operations.

We used this rock physics model in a relative manner for our interpretations of the time-lapse 3D seismic and P-SV data. This will be described in the following sections.

Seismic calibration and interpretation

The 2002 baseline data were used as a reference data set, and the 2006 monitoring data were calibrated to the 2002 data to remove differences between them that were not production-related response changes.

Figure 2 shows the final migration of the NS line from both the 2002 and 2006 surveys. Calibration has not yet been applied. The southern half of this line intersects with the SAGD well pairs H, I, K, L, M, and N; the northern part of the line is away from the steam-injected areas. Although Figure 2 shows remarkable changes in seismic response (around and below the red oval), there were also some differences to be compensated for between the two sections with regard to frequency contents and static shifts.

Figure 3 compares the calibrated 2006 data with the 2002 data. Our calibration consisted of band-pass filter, trace scaling, phase-and-amplitude correction and static time correction.

Figure 4, our interpretation of the line, clearly shows time delays of seismic events at the reservoir bottom (Top Devo-

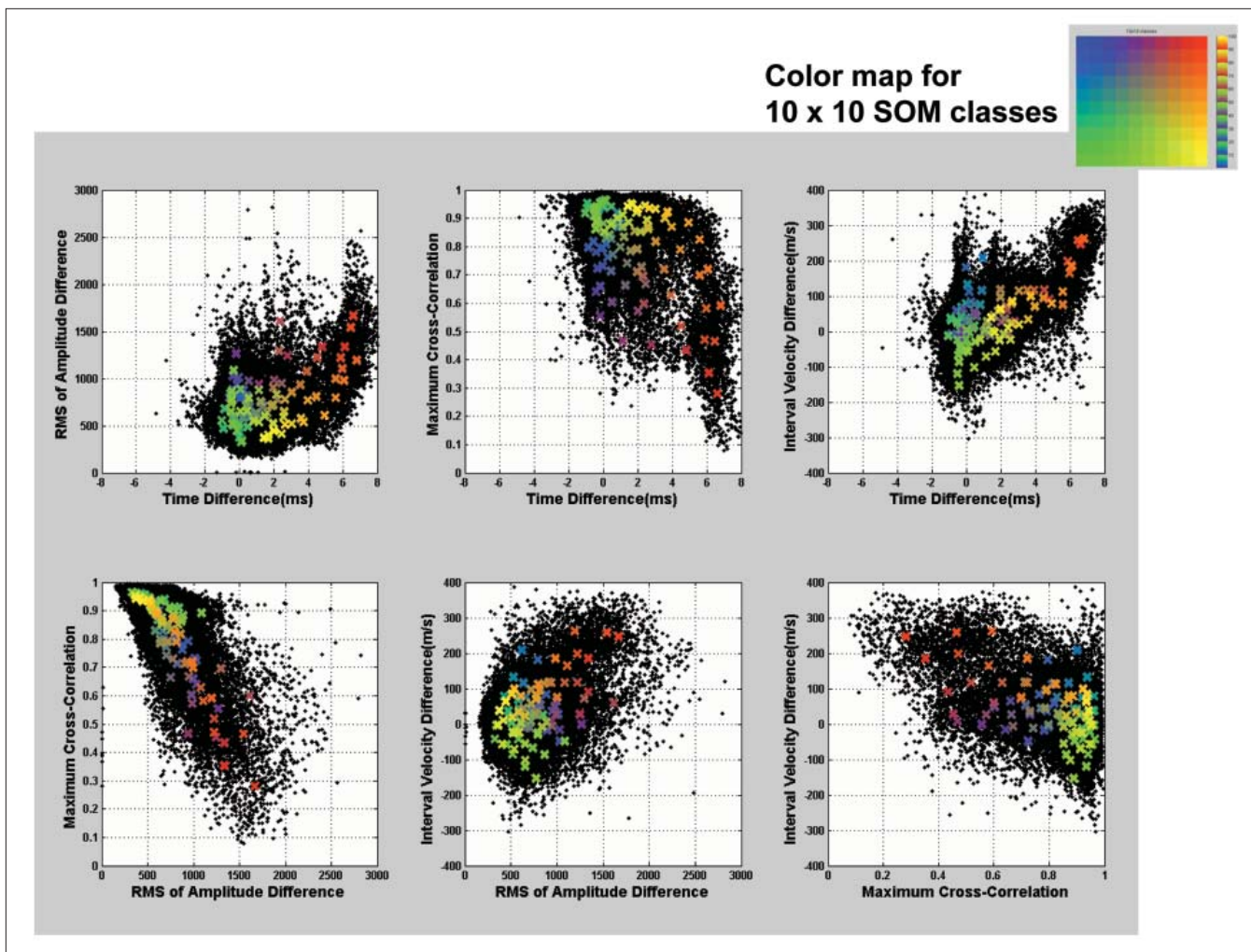


Figure 10. Crossplots between the four map attributes with their SOM prototype vectors. Black dots are raw attribute data and colored crosses show the SOM prototype vectors (100 classes). Close prototype vectors in the SOM domain have similar colors.

nian) and below the reservoir around the active SAGD well pairs which passed through the left half of each section.

Figure 5 shows a time-difference map between the Top Devonian horizons of the 2002 and the 2006 data. As reservoir thickness did not change due to the steam-injection, positive traveltimes differences in Figure 5 represent the V_p decreases within the reservoir. Significant V_p decreases in the oil-sands layer were observed around the SAGD well pairs in the western part of the survey area. As stated before, the production of the five eastern well pairs (A, B, C, D, and E pairs) had already started when the baseline survey was recorded. Therefore, the reservoir property changes between the two surveys were relatively small in the eastern areas.

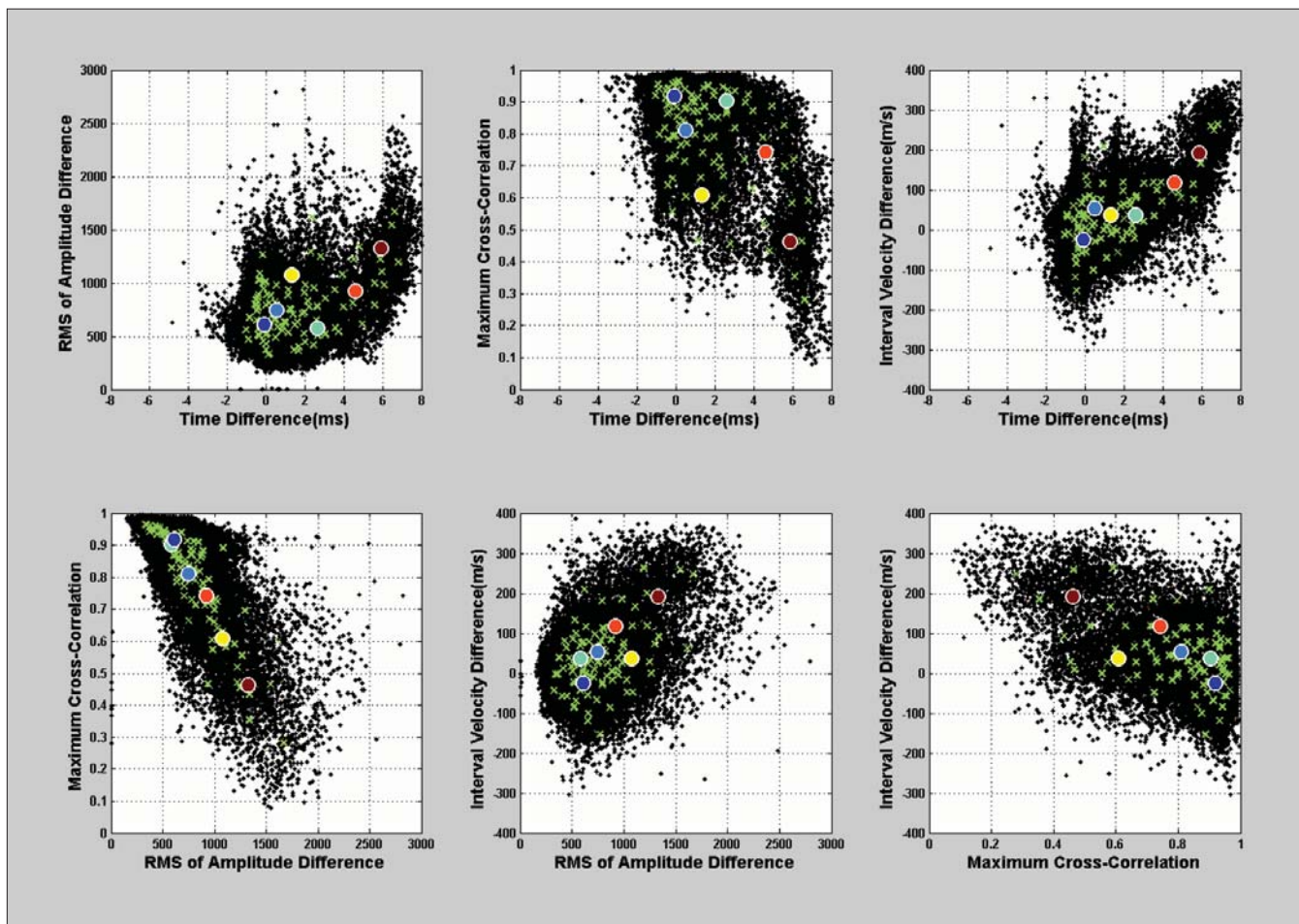
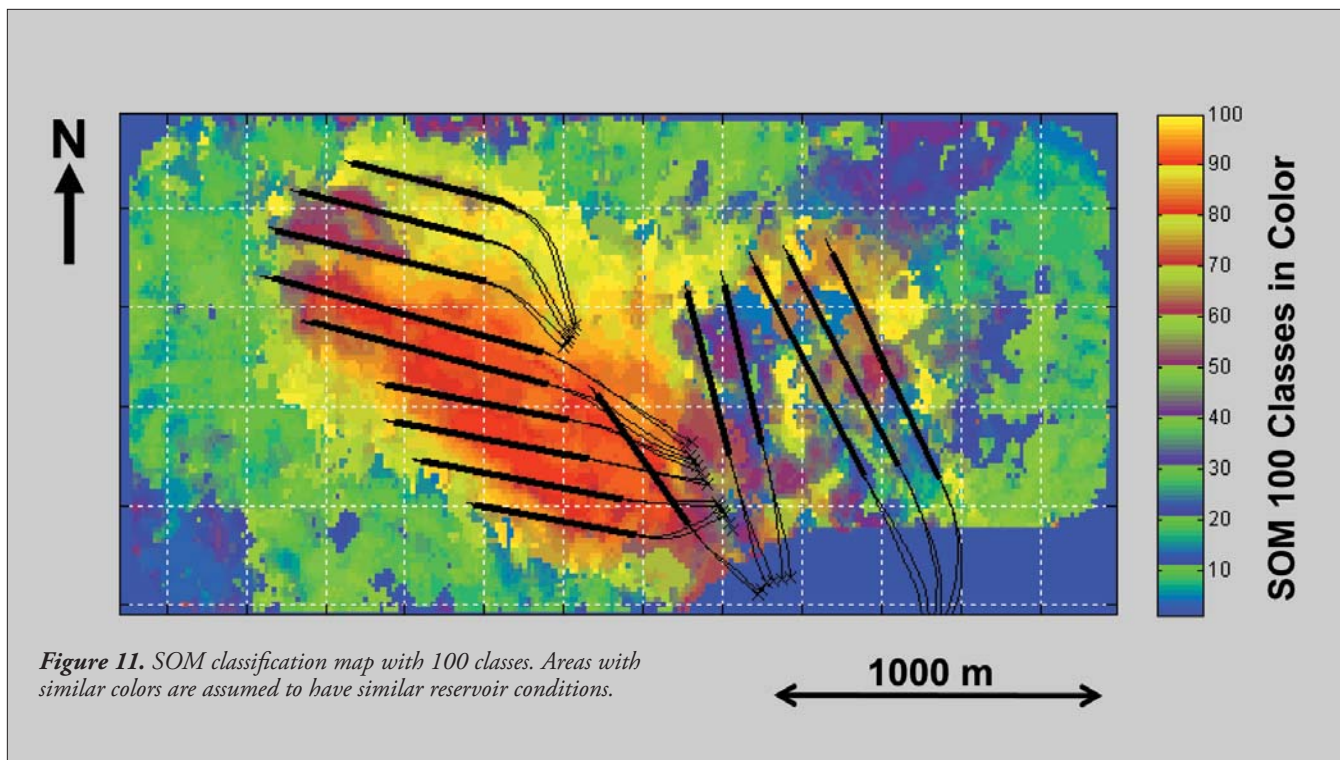
Figure 4 also shows large differences in seismic character within the reservoir around the active SAGD well pairs. To analyze seismic response changes (such as amplitude) within the reservoir, we applied a horizon-based time-shift correction to the 2006 data. This correction means the times of the 2006 interpreted horizons were adjusted to their corresponding 2002 horizons in a “stretch and squeeze” manner to remove production-related time delays (Figure 6).

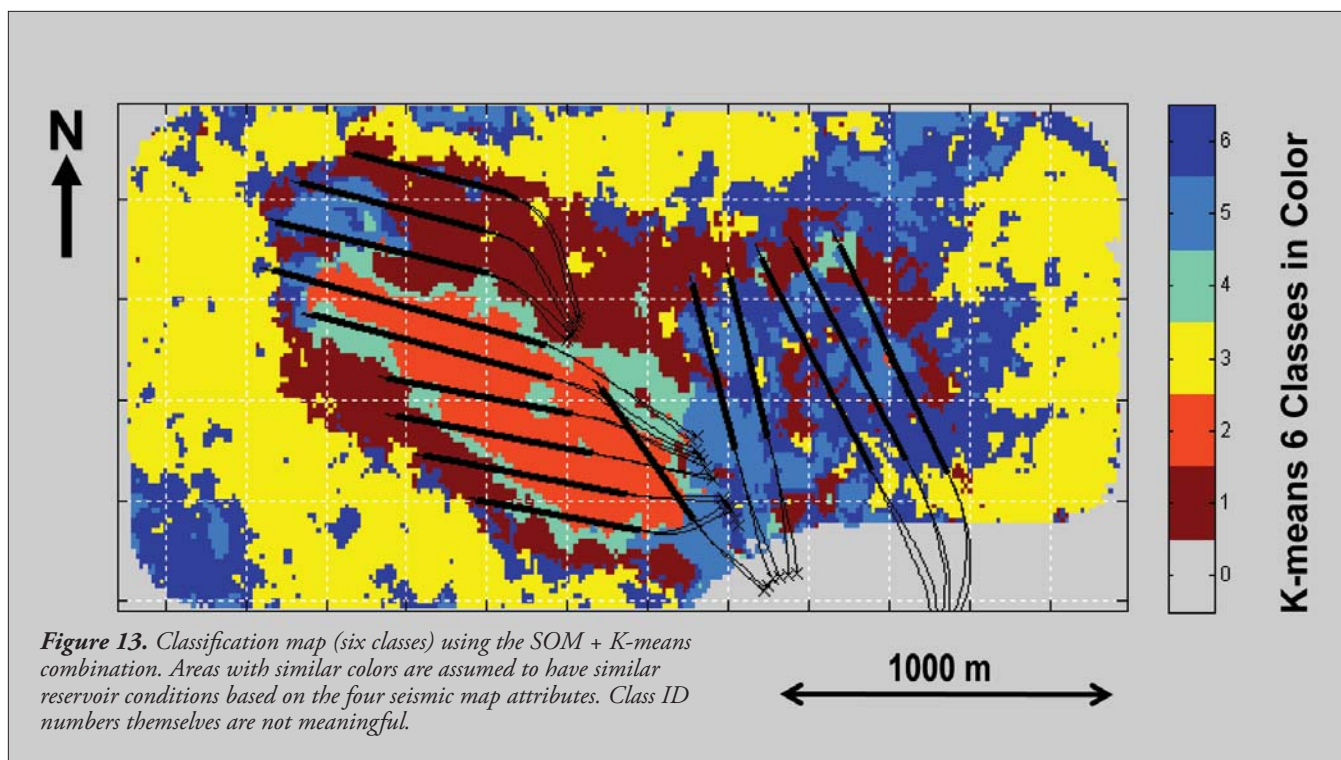
We calculated trace shape similarity and amplitude differ-

ence within the reservoir between the two data volumes on a trace-by-trace basis. Figure 7 and Figure 8 can be considered trace shape similarity maps that show maximum cross-correlation values and rms values of amplitude differences within the reservoir on each trace location, respectively. Around the ten western SAGD well pairs, Figure 7 shows low cross-correlation areas (green to magenta) and Figure 8 shows dominant high-amplitude difference areas (red to dark red). These low-similarity areas indicate production-related trace shape changes in the field.

Detailed velocity analysis at every CMP location using two 3D seismic prestack gather data sets also was conducted in order to detect small P-wave velocity changes within the oil-sands reservoir caused by the steam injection. Figure 9 is a time slice intersecting the reservoir showing interval velocity differences between the 2002 and 2006 smoothed interval velocity cubes.

As Figures 5, 7, 8, and 9 are quite consistent with each other, these four maps were integrated into one map using SOM (self-organizing maps) (Kohonen, 2001) and K-means methods (Matos et al., 2007) to analyze regional seismic characteristics. These are effective methods for nonsupervised clustering analysis using seismic attributes.





Our basic procedure for integrating the four maps is as follows: first, four-dimensional vector space consisting of (1) time difference, (2) maximum cross-correlation, (3) rms value of amplitude difference, and (4) interval velocity difference was assumed. The number of vectors therefore is equal to the number of CMP bins. Next, prototype vectors (representative vectors calculated from the data) were selected by the SOM technique. Assuming the number of the prototype vectors to be 100, the 100 prototype vectors were defined, each input four-dimensional vector was grouped into the nearest prototype vector, and then all the input vectors were classified into 100 classes. These 100 classes can be assumed to represent 100 patterns of reservoir change. Finally, the 100 SOM prototype vectors were classified into six classes by the K-means method to reduce the class number, and then the original input four-dimensional vectors were grouped into their nearest SOM + K-means prototype vector.

Figure 10 show crossplots between the four map attributes with their SOM 100 prototype vectors. Figure 11 shows an SOM classification map.

Figure 12 shows crossplots between the four map attributes with their classification by the SOM and SOM + K-means methods. Figure 13 is a classification map using the SOM + K-means combination method showing the clustering of the data of the four-attribute vectors into the six groups.

Figure 11 and Figure 13 can classify the extent of the rock property changes caused by the steam-injection into 100 classes and six classes, respectively. In Figure 11, steam chambers were considered to have grown sufficiently in the red and orange areas, but did not develop in the green and blue areas. We also consider that yellow areas in Figure 11 indicate tran-

sition zones. In Figure 13, our interpretation was that steam chambers grew sufficiently in the orange and cyan areas (class ID = 2 and 4), but did not develop in the yellow and blue areas (class ID = 3 and 6). We also consider that brown areas (class ID = 1) indicate the transition zones.

Since SAGD operation of the five eastern well pairs (A, B, C, D, and E pairs) started before the baseline seismic survey, and the reservoir property changes around them were relatively small, it is difficult to interpret the rock property changes on those areas. The integrated maps like Figure 11 and Figure 13, however, help qualitatively delineate the steam-affected zones.

Spectral decomposition

Spectral decomposition, based on a wavelet-transform method, was conducted to detect detailed changes of the spectrum components of the seismic data due to the steam injection.

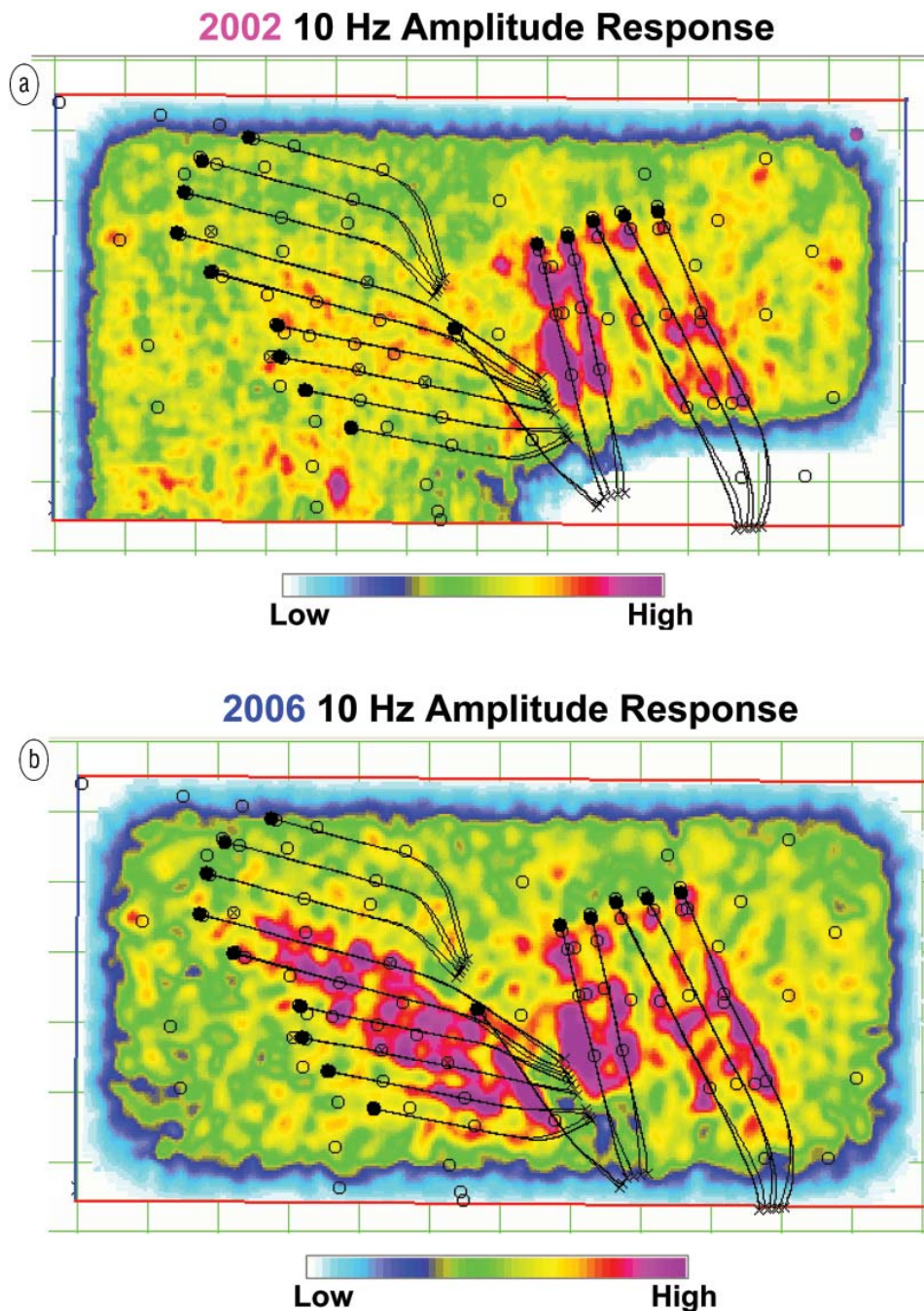
Figures 14a and 14b show time slices of 10-Hz isofrequency amplitude spectrum cubes for the 2002 and 2006 data, respectively. The 10-Hz isofrequency amplitude cube is composed of the 10-Hz component value of the amplitude spectrum calculated at each time sample. The maps in Figure 14 show noticeable seismic anomalies around the active SAGD wells at each survey time and enable us to qualitatively delineate the steam-affected zones.

P-SV analysis and interpretation

P-SV seismic data processing using the three-component 2006 seismic data was conducted to characterize the oil-sands reservoir using V_p and V_s information simultaneously.

First, we carried out modeling of the P-SV and P-P seismic responses with the well-log data. Figure 15 shows the

Figure 14. Time slices from spectral amplitude cubes at 10 Hz of (a) the 2002 3D seismic data, and (b) the 2006 3D seismic data. These time slices are within the reservoir interval. Warm colors mean higher amplitude values, and cold colors represent lower values.



P-SV and P-P synthetic seismograms (angle gathers) at a well located outside the steam-affected areas. Next, the synthetic P-P and P-SV reflection events were correlated with the well markers, and then the P-P and P-SV synthetic data were tied to the P-P and P-SV seismic data. Figure 16 shows an example of the time sections. Three horizons (including Top Devonian and Top Wabiskaw) are shown on the P-SV and P-P sections.

Figure 17 shows the V_p/V_s ratio map between Top Wabiskaw and Top Devonian horizons based on the P-P and P-SV data. The V_p/V_s ratios were calculated using the following formula:

$$\frac{V_p}{V_s} = \frac{2TWT_{PSV} - TWT_{PP}}{TWT_{PP}}$$

where TWT_{PSV} and TWT_{PP} are the P-SV isochron and P-P isochron, respectively, between the two horizons.

As the majority of the interval between Top Wabiskaw and Top Devonian corresponds to the reservoir zone in steam-injected area, the V_p/V_s ratio of that interval approximately represents the V_p/V_s ratio of reservoir zone. Figure 17 also shows comments regarding the V_p/V_s ratio. On this map, we classified the areas with visually high or low V_p/V_s ratios

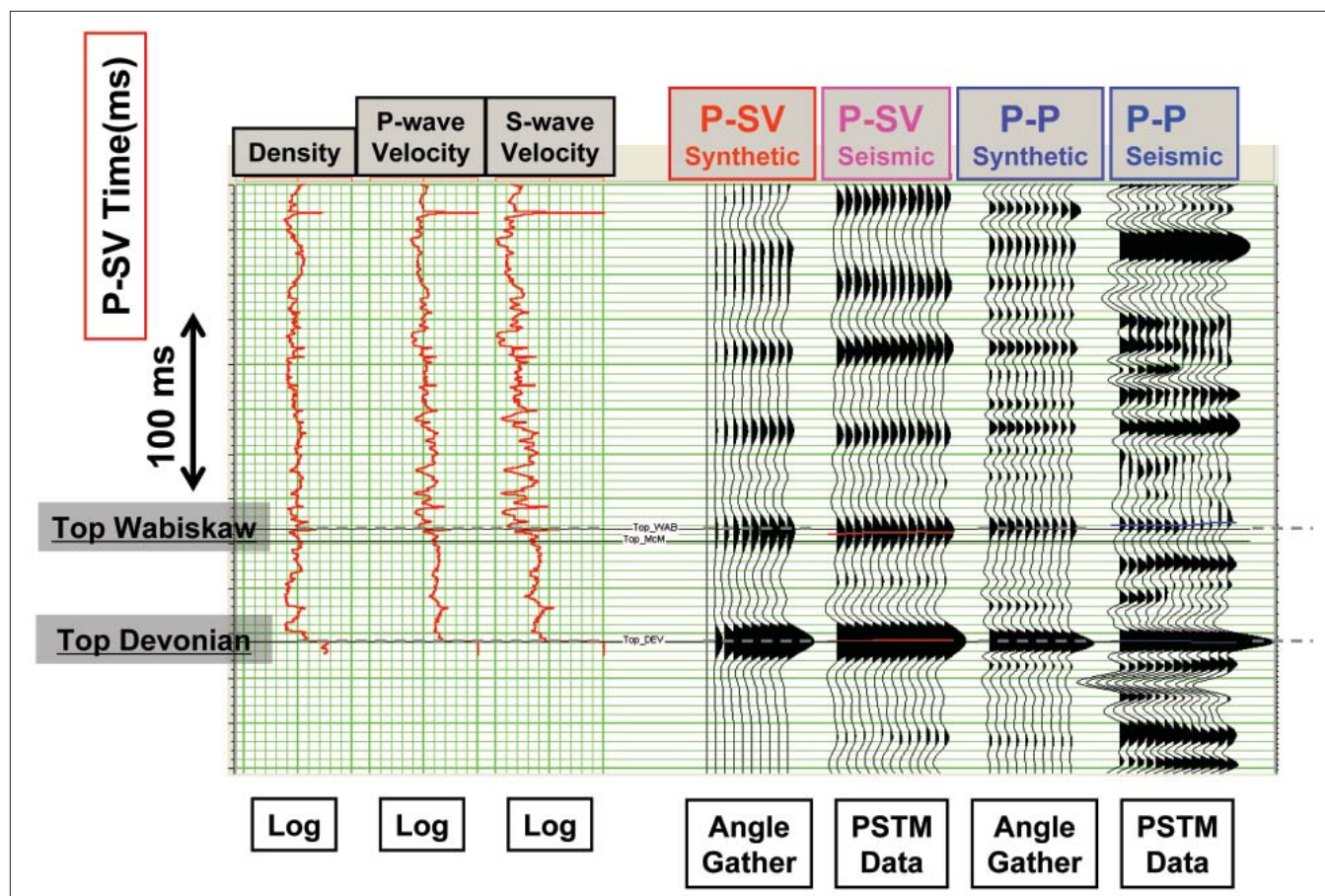


Figure 15. Example of the P-SV and P-P synthetic seismograms (angle gathers) with density log, V_p log, V_s log, and both the 2006 PSTM P-SV and the 2006 PSTM P-P seismic sections around the well. Time scale is P-SV time domain.

into three groups (note that our qualitative interpretation of Figure 17 was done in combination with the results of Kato et al. which are described in the companion article in this *TLE* special section):

- 1) Areas with low V_p/V_s ratios (enclosed by black dashed polygons around A, B, C, D, E, H, I, J, and K well pairs) are ones in which the steam chamber grew sufficiently. These low V_p/V_s ratio areas were probably under the conditions around step 21 as described by Kato et al.
- 2) Areas of high V_p/V_s ratios surrounded by white dashed polygons (in front of the toe of well pair H and between well pairs J and O) are probably steam-affected, but the steam chambers did not develop sufficiently. Although the steam chambers partly developed, the reservoir conditions of these high V_p/V_s ratio were, on the whole, somewhere in the high V_p/V_s ratio steps—step 6 through step 20 in Kato et al.
- 3) Areas of high V_p/V_s ratios enclosed by brown dashed polygons (in front of the toes of the I, J, and N well pairs) were little affected by steam as these areas are known from well data to have poor reservoir development.

The interval V_p/V_s ratio information is useful for estimation of the rock property changes of the oil-sands reservoir.

We, however, have to consider that the zone used for the V_p/V_s ratio calculation was thicker than the real oil-sands reservoir interval, and the V_p/V_s ratio map did not show the accurate V_p/V_s values of the reservoir itself. Thin shale layers within the reservoir were also neglected and the reservoir interval was treated as one homogeneous oil-sands layer. This is mainly because the temporal resolution of the P-SV data was much lower than the P-P seismic data, and it was too difficult to interpret the horizons within the reservoir in detail. V_p/V_s ratio maps such as Figure 17 are, however, qualitatively valuable for estimating reservoir properties.

Discussion

As stated before, Figures 5, 7, 8, and 9 are qualitatively consistent with each other especially around the ten western SAGD well pairs. However, when these maps are compared in detail, some inconsistencies between the edges and the shapes of the anomaly areas on these maps were noted. Our interpretations of the inconsistencies using our rock physics model are as follows:

- Large velocity decreases should occur in the high-temperature zone in the steam chamber, and smaller velocity decreases are predicted in the high pore-pressure zone based on our rock physics model.

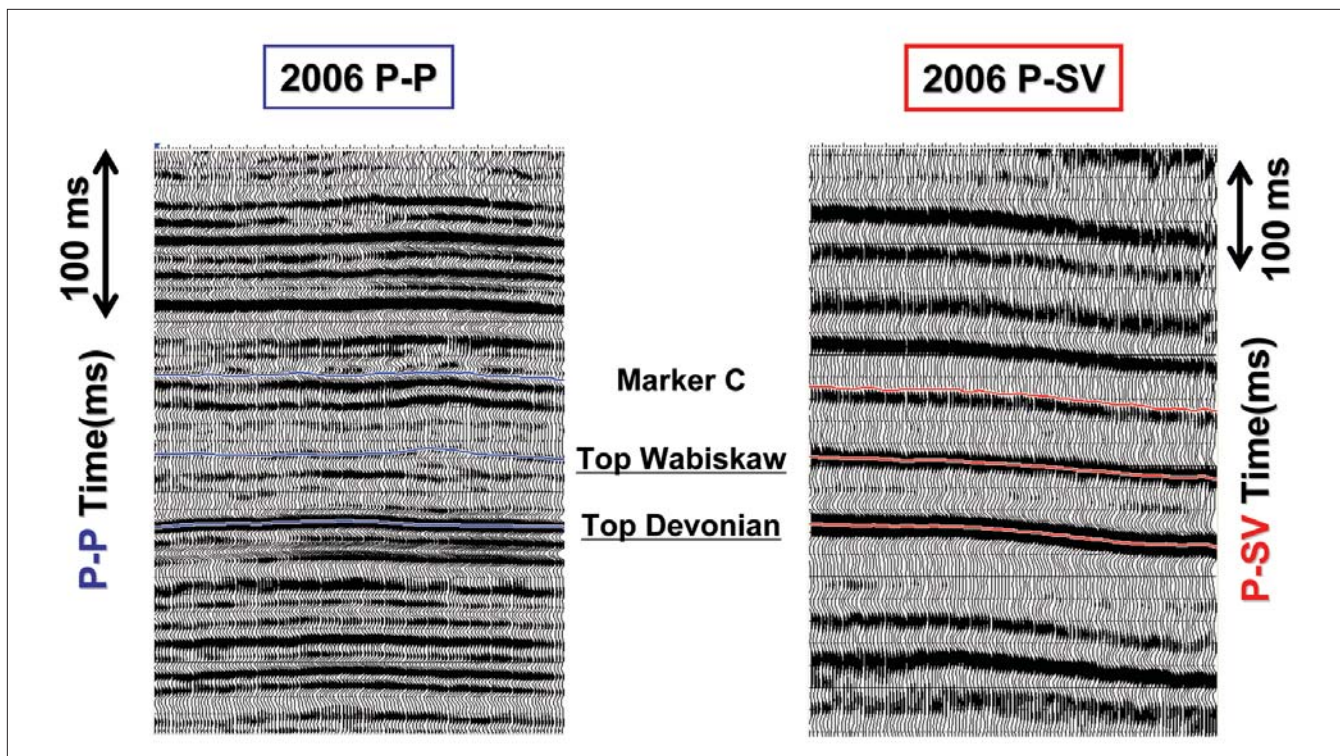


Figure 16. Example of the P-SV and P-P time sections along a sample line with three horizons including Top Devonian, Top Wabiskaw, and another seismic event. Time scales of the two sections are different.

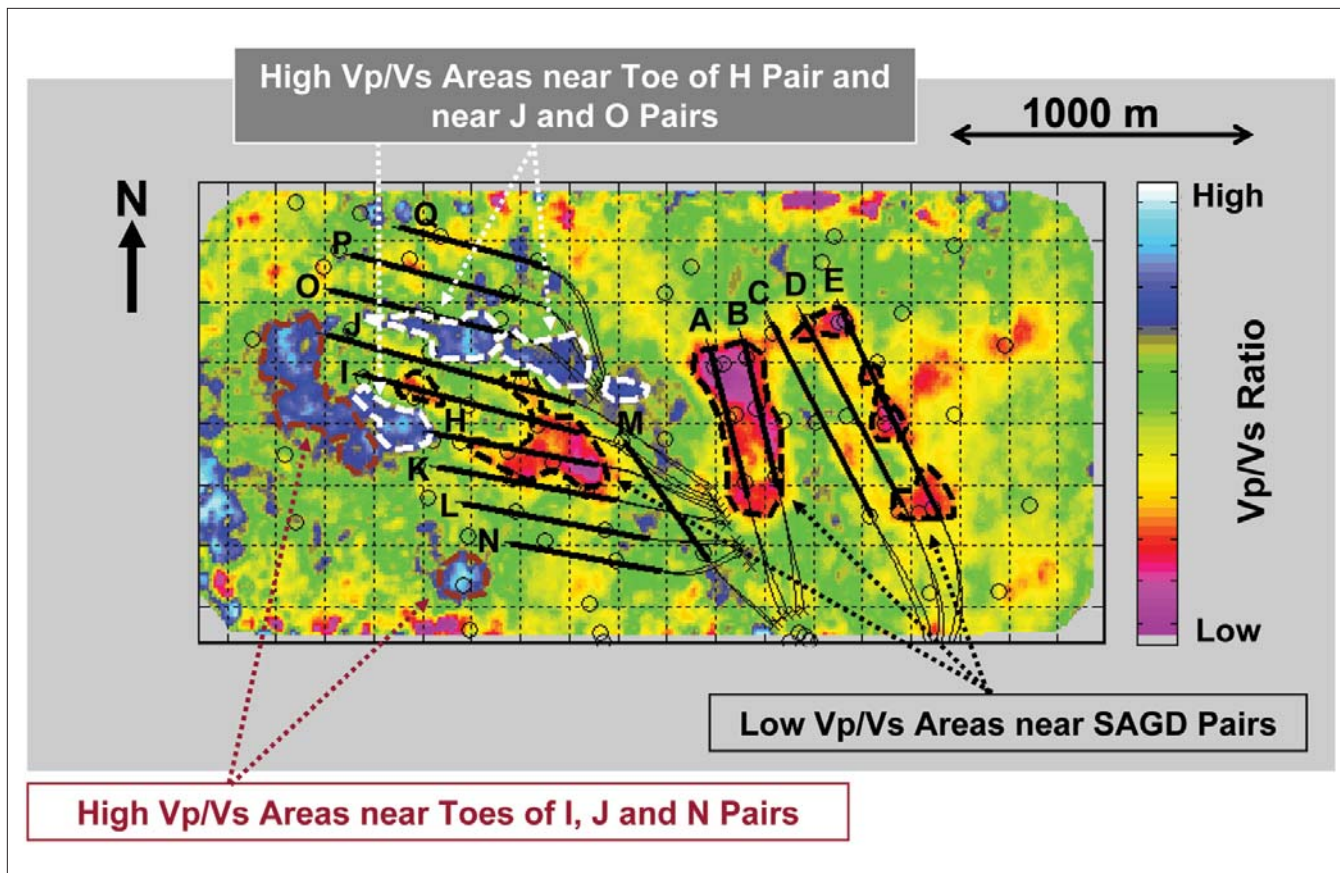


Figure 17. Interval V_p/V_s ratio map between Top Wabiskaw and Top Devonian horizons. Warm colors represent lower V_p/V_s ratios and cold colors mean higher V_p/V_s ratios. Areas with high or low V_p/V_s ratios were selected and classified into three groups. Each group was annotated with an individual color, and the area of each group was outlined with a colored dashed line.

- Thermal conductivity of the oil sands is so low that the heat front is relatively close to the steam chamber front. Conversely, the pressure fronts are expected to spread wider than the heated zones. As a result, a larger area would be influenced by pressure than by temperature.
- Large time delays of the Top Devonian horizon and large trace shape changes in the reservoir are expected in the extent of the steam chamber zones, and small time delays of the Top Devonian horizon and small trace shape changes in the reservoir are expected in the extent of the pore pressure increase zones. Currently we consider that Figure 5 basically shows anomalous areas caused by the combination of high temperature and high pore pressure, and Figures 7, 8, and 9 mainly represent areas heated during the time between the two seismic surveys.

Conclusion

The time-lapse seismic survey and analysis were conducted in the JACOS Hangingstone SAGD operations area to monitor steam chamber development. The two seismic P-P volumes acquired in 2002 and 2006 show large differences in seismic character within the reservoir around the SAGD well pairs, and the V_p/V_s ratio map from the P-SV and P-P volumes of

the 2006 three-component data clearly shows areas of variation.

The time-lapse seismic monitoring and the P-SV seismic data are useful for investigating the rock property changes of the interwell reservoir sands in the field. The results of the geophysical study are now being integrating with geological and production information for efficient reservoir management.

Suggested reading. “Elastic property changes of bitumen reservoir during steam injection” by Kato et al. (*TLE*, 2008). *Self-Organizing Maps* by Kohonen (Springer-Verlag, 2001). “Unsupervised seismic facies analysis using wavelet transform and self-organizing maps” by Matos et al. (*GEOPHYSICS*, 2007).

TLE

Acknowledgements: This study was conducted jointly between Japan Canada Oil Sands Limited (JACOS) and Japan Oil, Gas and Metals National Corporation (JOGMEC). The authors thank JOGMEC, JACOS, and JAPEX for permission to publish these data.

Corresponding author: toru.nakayama@japex.co.jp